Advanced Si-based Gate Stacks

Mater. Res. Soc. Symp. Proc. Vol. 1155 © 2009 Materials Research Society 1155-C12-01

Defects in HfO_2 Based Dielectric Gate Stacks

Patrick M. Lenahan[1], Jason T. Ryan[1], Corey J. Cochrane[1], and John F. Conley Jr.[2]

[1]The Pennsylvania State University, University Park, PA 16802, U.S.A.

[2]Oregon State University, Corvallis, OR 97331, U.S.A.

ABSTRACT

We report on both conventional electron paramagnetic resonance (EPR) measurements of fully processed HfO_2 based dielectric films on silicon and on electrically detected magnetic resonance (EDMR) measurements of fully processed HfO_2 based MOSFETs. The magnetic resonance measurements indicate the presence of oxygen vacancy and oxygen interstitial defects within the HfO_2 and oxygen deficient silicons in the interfacial layer. The EDMR results also indicate the generation of at least two defects when HfO_2 based transistors are subjected to significant negative bias at modest temperature. Our results indicate generation of multiple interface/near interface defects, likely involving coupling with nearby hafnium atoms.

INTRODUCTION

Tremendous progress has been made towards replacing conventional (SiO_2 and SiO_xN_y) gate dielectrics with HfO_2 based materials in high performance metal-oxide-silicon (MOS) field effect transistors (MOSFETs) [1, 2]. However, there are many challenges in the integration of these materials into MOS technology. Critical issues include: trapping in HfO_2 [3, 4], trapping in the interfacial layer dielectric between the silicon and the HfO_2 [5, 6], silicon/dielectric interface traps [1] and various instabilities which may involve either the generation of new traps or the population of existing traps or both of these processes [7].

Magnetic resonance techniques, such as conventional electron paramagnetic resonance (EPR) or electrically detected magnetic resonance (EDMR) techniques such as spin dependent recombination (SDR), are the most powerful tools currently available to identify the structure of these trapping centers [8]. The technique is generally sensitive to paramagnetic defects. (Nearly all electrically active defects can be rendered paramagnetic.) Information about the local structure of trapping defects can be gleaned from the relationship between the magnetic field and microwave frequency at which resonance occurs. In the simplest of cases, the resonance condition is given by [8],

$$h\nu = g\beta H, \qquad (1)$$

where h is Planck's constant, ν is the microwave frequency, β is the Bohr magneton, H is the magnetic field and g is number, typically close to 2, which depends upon the relationship between the defect's orientation and the magnetic field vector. The g is expressed in terms of a matrix which is often called the g tensor. (This simple relationship is often altered by the presence of nearby magnetic nuclei and other factors which will not be particularly relevant for the results presented in this paper.)

HfO_2 DEFECTS

At least two intrinsic defects have been observed in magnetic resonance observations of HfO_2 films on silicon: oxygen vacancies and oxygen interstitials. Kang et al.[9] and Ryan et al [10]. reported the generation of two strong signals in HfO_2 films subjected to, respectively, vacuum ultraviolet (VUV) illumination under bias and gamma irradiation. (Ryan et al. [10] also reported the generation of P_b like Si/dielectric interface traps.) Figure 1 illustrates a post- VUV EPR trace and figure 2 illustrates pre- and post- gamma irradiation traces. (The spectrometer settings are slightly different in the VUV and gamma irradiation traces; in addition, the generation of P_b centers in the gamma irradiation case somewhat alters the results of figure 2.) These representative results indicate the presence of oxygen vacancies and oxygen interstitials [9-11]. Figure 3 illustrates a comparison of a post VUV trace and a simulated EPR trace for a defect with g matrix components corresponding to $g_{zz} = 2.04$, $g_{yy} = 2.01$, and $g_{xx} = 2.000$. These g matrix components correspond closely to the well established components for oxygen interstitials observed previously in quite similar materials such as ZrO_2. The signal on the far right of both traces were tentatively linked to an oxygen vacancy by Ryan et al. [10] and by Lenahan and Conley [11]. This somewhat tentative identification became more definitive with recent density functional theory calculations by Ramo et al. [12] who predicted that a (positively charged) oxygen vacancy would have a g matrix corresponding to $g_{xx} = 1.9835$, $g_{yy} = 1.963$, and $g_{zz} = 1.9450$. Figure 4 illustrates a comparison of the right side signal trace in figures 1 and 2 with that of a calculated trace utilizing the Bruker Biospin SimFonia software and the g matrix components calculated by Ramo et al. [12] The higher broadening trace is an excellent match to the experimental data. (The low broadening trace indicates that, at the very least, the center of the spectrum and its approximate width agree with the Ramo et al. calculations.) Figure 5 illustrates a comparison of the data from figures 1 and 2 and a simulation of the sum of the oxygen interstitial and oxygen vacancy centers, again utilizing the Bruker Biospin SimFonia software. The agreement between the simulation and the data is quite close. The observations of oxygen vacancies and oxygen interstitials as dominating HfO_2 defects is generally consistent with several "theoretical" studies of HfO_2 defects [13, 14].

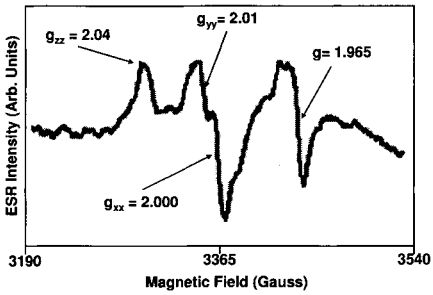

Figure 1. An EPR trace taken on an HfO_2 film on silicon which has been subjected to vacuum ultraviolet illumination $hc/\lambda < 10.2eV$ under negative gate bias. The illumination resulted in an electron fluence of approximately $2x10^{13}$ cm^{-2} in the "bulk" of the film and a comparable hole fluence near its surface. The trace indicates the presence of high densities ($> 10^{12}$ cm^{-2}) of oxygen vacancies and oxygen interstitials.

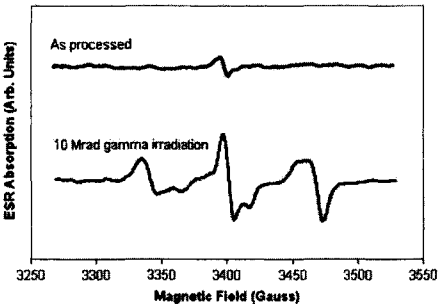

Figure 2. Pre-irradiation (above) and post-irradiation (below) wide scan ESR traces indicating the generation of several defects in the $Hf(NO_3)_4$ precursor HfO_2 dielectric film on H-terminated silicon. The two peaks on the left are (mostly) due to an O_2^- coupled to a hafnium ion (the central peak includes a small contribution from P_b centers). The peak on the far right is likely due to an oxygen vacancy in the HfO_2. In these traces, the spectrometer settings have been set to optimize the O_2^- and oxygen vacancy spectra. The post irradiation trace indicates the presence of high densities ($>10^{12}$ cm^{-2}) of both oxygen vacancies and oxygen interstitials.

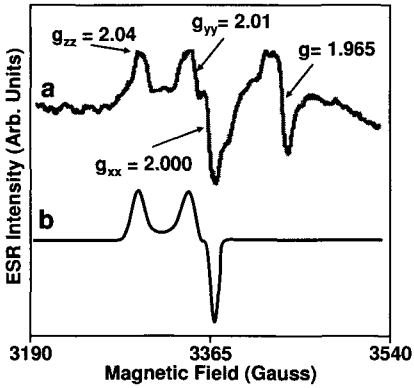

Figure 3. (a) EPR trace generated by VUV illumination under bias compared to the (b) simulated EPR spectra with g_{xx} = 2.04, g_{yy} = 2.01, and g_{zz} = 2.000.

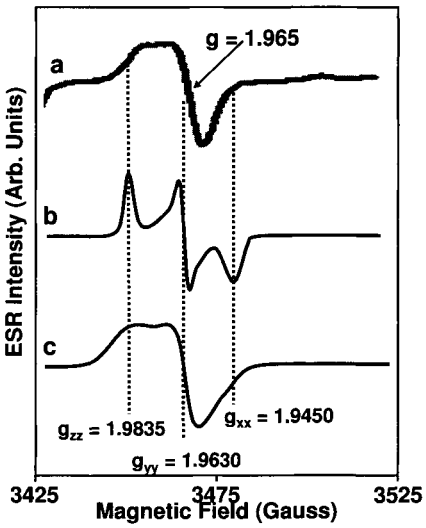

Figure 4. (a) EPR data from Ryan et al. [10], (b) positive oxygen vacancy spectrum simulation with low broadening, and (c) positive oxygen vacancy spectrum simulation with high broadening. In both simulations, the g matrix calculations of Ramo et al. [12] were utilized.

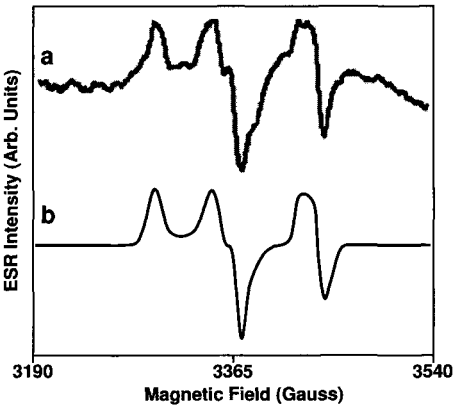

Figure 5. (a) EPR data from Kang et al. [9] and (b) simulation of the positive oxygen vacancy and oxygen interstitial. The simulation is based on the sum of simulations in figures 3 and 4.

DEFECTS IN THE INTERFACIAL LAYER

Ryan et al. [15, 16] and Bersuker et al. [17] have reported the observation of several E' center variants in the interfacial layer of HfO_2 based structures. (E' centers are oxygen deficient silicons, dominating deep level defects in conventional SiO_2 based oxides. Their EPR spectra are characterized by narrow lines with zero crossing g values between 2.000 and 2.003.) Ryan et al. [15, 16] and Bersuker et al. [17] noted a very strong processing dependence of these defects in the interfacial layer. Figures 6 and 7 illustrate this strong process dependence.

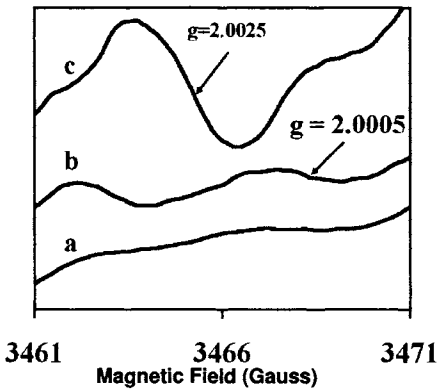

Figure 6. Comparison of three very differently processed samples; (a) 3 nm HfO_2 deposited on etch-back in-situ steam generated SiO_2, (b) a sample identical to (a) except that it received a 700 and 1000°C N_2 post deposition anneal, and (c) a sample identical to (b) except that it had a 10nm thick TiN cap deposited prior to N_2 annealing.

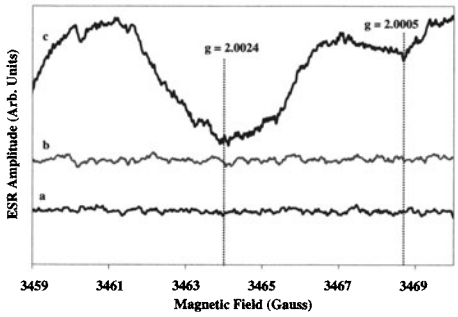

Figure 7. Three second derivative EPR traces of (a) control 1nm ozone grown SiO_2, (b) 3 nm HfO_2 deposited on 1nm ozone grown SiO_2, and (c) oxygen deficient HfO_2 deposited on 1nm ozone grown SiO_2. Note that the deposition of the oxygen deficient HfO_2 film grossly increases the densities of the two E' like signals.

Ryan et al. [15] also noted that these interfacial E' variants exist in an environment which cannot be fully amorphous or a non textured polycrystalline matrix. They showed that this must be so because the spectrum depends on the orientation of the device structures in the magnetic field. This is illustrated in figure 8.

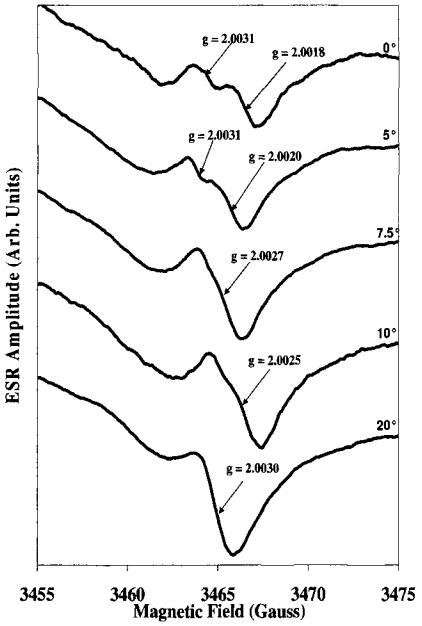

Figure 8. EPR vs. sample orientation. Note the change in line shape as the sample is rotated in the applied magnetic field. This demonstrates that the defect cannot reside in a purely amorphous or non-textured polycrystalline matrix.

Ryan et al. [15] also showed that the amplitude of these E' signals depends upon the position of the silicon/dielectric Fermi energy. This result demonstrates that the centers can act electronically as interface traps. This result is illustrated in figure 9. As the Fermi level passes up and through the silicon/dielectric interface band gap, the centers can pick up first one electron, rendering the center paramagnetic (EPR active) and then a second electron rendering the defect diamagnetic (EPR inactive). Since these centers have also been observed in HfO_2 and hafnium silicate structures by at least two groups [18, 19], sometimes at high density, it is likely that they are performance limiting defects of widespread importance.

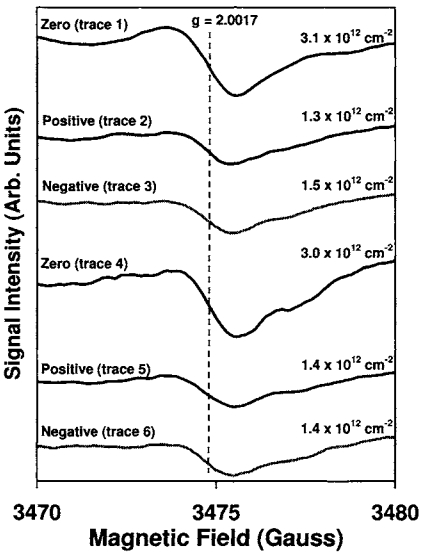

Figure 9. ESR vs. applied gate bias. Note the amplitude modulation as a result of biasing. The defect acts as both an electron and hole trap.

INTERFACE/NEAR INTERFACE DEFECTS GENERATED IN BIAS TEMPERATURE INSTABILITIES

Cochrane et al. [20] have reported on the generation of interface/near interface defects in fully processed HfO_2 based transistors subjected to negative bias stressing at room temperature and elevated temperature. The key results are illustrated in figures 10, 11, and 12. Figure 10 illustrates gated diode (DCIV) recombination current measurements on an unstressed transistor, a transistor subjected to brief room temperature negative bias stress, and a more lengthy negative bias stress. The amplitude of the DCIV peak scales with the density of interface traps. Figure 11 illustrates pre- and post- room temperature stressing EDMR measurements obtained by SDR. Figure 12 illustrates pre- and post- high temperature stressing SDR measurements. Note that rather broad SDR spectrum with a different zero crossing g values. The short room temperature stressing SDR response g = 1.9998; the long high temperature stressing SDR response g = 2.0026. The post high temperature stressing SDR spectrum is significantly narrower than the room temperature stressing signal. Figure 13 compares long time high temperature negative bias stressed HfO_2 device response to the response of a similarly stressed plasma nitrided SiO_2 (PNO) device and a SiO_2 device. As reported elsewhere, in SiO_2 devices, the process is dominated by P_b centers [21]; in PNO devices, the process is dominated by K centers [22], silicons back bonded to three nitrogen atoms. The SDR results on the HfO_2 results demonstrate that the NBTI defects in these devices are clearly different than those in conventional SiO_2 and PNO devices.

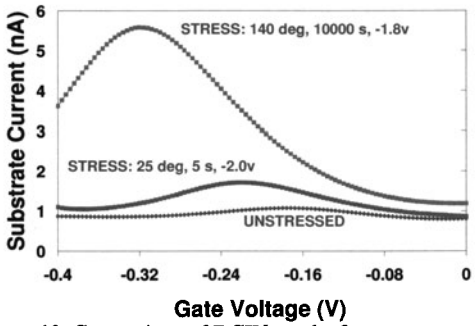

Figure 10. Comparison of DCIV results for an unstressed device, a device subjected to a 5s room temperature stress (25 °C at –2.0 V), and a device subjected to extended stressing at an elevated temperature (140 °C at –1.8 V for 10 000 s).

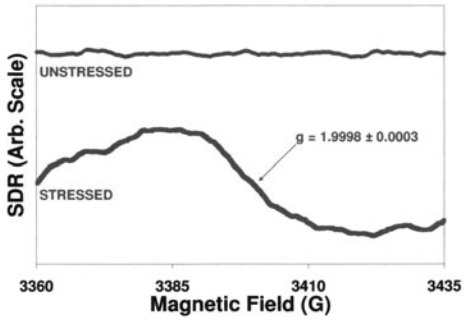

Figure 11. SDR results for an unstressed and 5s room temperature negative bias stressed device (25 °C and –2.0 V). SDR was performed on this device with a gate voltage of –0.220 V. The g of 1.9998 corresponds to a microwave frequency ν = 9.5165 GHz and magnetic field H=3400 G.